BNL-71727-2003-JA

ELSEVIER

Aerosol Science 35 (2004) 577–598

Journal of
Aerosol Science

www.elsevier.com/locate/jaerosci

Representation of generally mixed multivariate aerosols by the quadrature method of moments: II. Aerosol dynamics

Choongseok Yoon[a,b,1], Robert McGraw[a,*]

[a] *Atmospheric Sciences Division, Brookhaven National Laboratory, Building 815E, Upton, NY 11973, USA*
[b] *Department of Applied Mathematics & Statistics, State University of New York, Stony Brook, NY 11794-3600, USA*

Received 28 July 2003; received in revised form 3 November 2003; accepted 5 November 2003

Abstract

The quadrature method of moments (QMOM) is extended to generally mixed multicomponent particle populations using principal component analysis (PCA). The resulting PCA-QMOM provides a versatile method for moment closure illustrated for generally mixed, multivariate, particle populations evolving under condensation, coagulation, sintering, and simultaneous processes. The method is illustrated using a 2^h-point quadrature version of the PCA-QMOM, where h is the number of coordinate dimensions, developed in the preceding paper (Paper I). Calculations for multiple particle populations interacting through coagulation are also presented. A theory is developed for the time-dependence of the covariance matrix of a multicomponent particle population evolving under a size-independent coagulation rate. It is found that the rank of the $h \times h$ covariance matrix, for h components, approaches unity at long time as the particle population evolves to an internally mixed, self-preserving size distribution state.
Published by Elsevier Ltd.

Keywords: Aerosol dynamics; Multicomponent aerosols; Moment methods; Principal component analysis; Multivariate; Quadrature

1. Introduction

In addition to particle mass loading, the chemical and physical properties of aerosols are determined by particle number density, composition, shape, and size distribution. In the atmosphere, particle number and composition control the indirect effects that aerosols have on climate through their

* Corresponding author. Tel.: +1-631-344-3086; fax: +1-631-344-2887.
E-mail address: rlm@bnl.gov (R. McGraw).

[1] Doctoral dissertation research carried out at BNL and SUNY-SB.

0021-8502/$ - see front matter Published by Elsevier Ltd.
doi:10.1016/j.jaerosci.2003.11.012

influence on cloud activation, drizzle production, and cloud radiative properties (Twomey, Piepgrass, & Wolfe, 1984; Albrecht, 1989; McGraw & Liu, 2003). Another example, again from the atmosphere, points to the mixing state of black carbon aerosols as having a significant influence on radiative forcing (Jacobson, 2001). The representation of such processes in models requires new multivariate approaches to aerosol simulation, which on account of the large numbers of variables involved will most likely have to be statistically based.

While particle populations of mixed shape and composition call for a multivariate description, the extreme computational requirements of multivariate particle distribution function (pdf) simulation have generally forced the use of zero dimensional (e.g. modeling sulfate mass), or univariate (e.g. modeling the pdf using a single radial or mass coordinate) approximations. Likewise, most treatments of multicomponent aerosols have been limited to the special cases of externally mixed or internally mixed particle populations. External mixtures are non-interacting particle populations, e.g. dust, sea salt, and sulfate in the atmosphere—to the extent that these are noninteracting—amenable to treatment using separate radius or mass coordinates for each population. Limited interactions between such populations (e.g. the aggregation of sulfate with the other particle types) have been accommodated within the univariate framework (Wright, McGraw, Benkovitz, & Schwartz, 2000), but the methods are not extendable to general mixtures. Internal mixtures, characterized by the property that all particles of the same total mass, m, have the same composition (Seinfeld & Pandis, 1998), are also amenable to a univariate treatment. Here the component species distributions are each represented as functions of particle mass. Sectional methods, which fractionate the pdf into discrete size classes, or sections, are naturally suited to the representation of internal mixtures (see for example Meng, Dabdub, & Seinfeld, 1998). Nevertheless, the computational demands are formidable even for univariate problems if a high-resolution description of the size distribution, requiring a large number of sections, is desired. Extensions of the modal (Wilck, 1998) and moment (McGraw & Wright, 2003) methods to internal mixtures have also been developed.

A recent extension of sectional methods to include multiple size distributions can in principle represent the intermediate (between internal and external) mixing states of the aerosol (Jacobson, 2002). The aerosol is partitioned into multiple distributions that are each characterized by their own sectional size coordinate. Coagulation, condensation, nucleation, and reversible chemistry are allowed to take place among the distributions. These results show the remarkable extent to which sectional methods can be developed using high speed computers. Limitations include the large number of variables that must be carried to represent the multiple size distributions. Additionally, only a sampling of the full pdf is obtained. The composition coordinates of the multiple size distributions must be assigned on a case-by-case basis prior to simulation, and these should be representative of the full compositional-coordinate space of the aerosol. At present, the assignment appears to require at least some degree of subjective model intervention.

In the previous paper (Part I) the quadrature method of moments (QMOM) was combined with principal component analysis (PCA) in a novel and very general way that makes explicit the statistical foundation of moment methods. This was achieved by adapting PCA to assign the quadrature points in higher dimension. The resulting PCA-QMOM is developed below to provide a computationally efficient, statistically based approach to multivariate aerosol dynamics simulation. The new methods are illustrated through simulations requiring the representation of generally mixed, multivariate, particle populations. These include multicomponent and mixed-shape particle populations evolving under typical aerosol microphysical processes including coagulation, sintering, and

condensation growth. Part I described the application of PCA to the QMOM with an arbitrary number of quadrature points per variable. The present paper (Part II) implements the method using two quadrature points per variable (e.g., 2^h quadrature points for an aerosol having h components).

2. Assignment of quadrature points by PCA

The multivariate mixed moments of an h-variate particle distribution function, $f(m_1, m_2, \ldots, m_h)$, are defined as

$$\langle m_1^p m_2^q \ldots m_h^w \rangle_f = \int\int \cdots \int m_1^p m_2^q \ldots m_h^w f(m_1, m_2, \ldots, m_h)\, \mathrm{d}m_1\, \mathrm{d}m_2 \ldots \mathrm{d}m_h, \tag{2.1}$$

where $\{m_i\}$ are the coordinates that characterize an individual particle, and $f(m_1, m_2, \ldots, m_h)$ gives the number of particles per unit volume having coordinate m_i between m_i and $m_i + \mathrm{d}m_i$ for all i. In most of the examples treated in this paper, m_i will be the mass of species i present in a multicomponent aerosol particle. In the bivariate model of Section 3.3, which describes nonspherical particles undergoing coagulation and sintering, m_1 and m_2 represent particle volume and particle surface area, respectively. PCA makes use of the probability density function, which is normalized to unity. Thus we will also require the moments of the normalized distribution $\tilde{f}(m_1, m_2, \ldots, m_h) = f(m_1, m_2, \ldots, m_h)/N_0$ where N_0 is the total number of particles per unit volume. These differ only by the factor $1/N_0$ from the moments of Eq. (2.1).

The calculations presented below are based on the most economical, 2^h-quadrature point, version of the PCA-QMOM, which tracks mixed-moments through second order, including the moments entering the covariance matrix. The present description is limited to this case. Extensions of the method to higher quadrature point densities, and correspondingly higher-order moments, is described in Paper I. Assignment of the 2^h points requires the following moments: the normalization $\langle 1 \rangle_f = N_0 \langle 1 \rangle_{\tilde{f}} = N_0$; the h coordinate means, $\langle m_i \rangle_{\tilde{f}} = \langle m_i \rangle_f / N_0$ for $i = 1$ through h; and the $h(h+1)/2$ distinct elements of the symmetric $h \times h$ covariance matrix, Σ:

$$\Sigma = \begin{pmatrix} \langle m_1^2 \rangle_{\tilde{f}} - \langle m_1 \rangle_{\tilde{f}}^2 & \langle m_1 m_2 \rangle_{\tilde{f}} - \langle m_1 \rangle_{\tilde{f}} \langle m_2 \rangle_{\tilde{f}} & \cdots & \langle m_1 m_h \rangle_{\tilde{f}} - \langle m_1 \rangle_{\tilde{f}} \langle m_h \rangle_{\tilde{f}} \\ \langle m_1 m_2 \rangle_{\tilde{f}} - \langle m_1 \rangle_{\tilde{f}} \langle m_2 \rangle_{\tilde{f}} & \langle m_2^2 \rangle_{\tilde{f}} - \langle m_2 \rangle_{\tilde{f}}^2 & \cdots & \langle m_2 m_h \rangle_{\tilde{f}} - \langle m_2 \rangle_{\tilde{f}} \langle m_h \rangle_{\tilde{f}} \\ \vdots & \vdots & & \vdots \\ \langle m_1 m_h \rangle_{\tilde{f}} - \langle m_1 \rangle_{\tilde{f}} \langle m_h \rangle_{\tilde{f}} & \langle m_2 m_h \rangle_{\tilde{f}} - \langle m_2 \rangle_{\tilde{f}} \langle m_h \rangle_{\tilde{f}} & \cdots & \langle m_h^2 \rangle_{\tilde{f}} - \langle m_h \rangle_{\tilde{f}}^2 \end{pmatrix}. \tag{2.2}$$

Thus the total number of moments required is $1 + h + h(h+1)/2 = (h^2 + 3h + 2)/2$. For specified values of these moments the assignment of quadrature points is straightforward, requiring only that the eigenvectors and eigenvalues of Σ be obtained. The eigenvectors, which are necessary to transform between coordinate systems, form the columns of an orthogonal matrix, $\mathbf{G}$, that transforms Σ to diagonal form. Thus $\mathbf{G}^{\mathrm{T}} \Sigma \mathbf{G} = \mathbf{D}$ where $\mathbf{G}^{\mathrm{T}}$ is the transpose of $\mathbf{G}$ and $\mathbf{D} = \mathrm{diag}(\lambda_i)$ is the diagonal matrix containing as its elements the eigenvalues of Σ. These are non-negative and ordered according decreasing size $\lambda_1 \geqslant \lambda_2 \geqslant \cdots \lambda_h \geqslant 0$. The eigenvalues give the variances of the probability

distribution function in the principal coordinate frame. Thus the largest variance is along the direction of the first principal coordinate, y_1: $\langle y_1^2\rangle - \langle y_1\rangle^2 = \lambda_1$. The second largest variance, along y_2, is given by λ_2, etc.

Having diagonalized Σ, the 2^h quadrature points are now trivial to assign in the principal frame. The transformed and centered coordinates of the abscissas are simply:

$$\{\pm\sqrt{\lambda_1}, \pm\sqrt{\lambda_2}, \pm\cdots\pm\sqrt{\lambda_h}\}. \tag{2.3}$$

The weights are identical and equal to $2^{-h}N_0$. It is convenient to number the quadrature points using a single index, j, which takes on values from 1 through 2^h. For example, a convenient mapping can be carried out by assigning the $\pm$ signs in Eq. (2.3) according to the pattern of 0's and 1's in the binary representation of $j-1$. In the absence of nonlinear variable transformations, of the kind described in Section 3.4 below, one is interested only in the quadrature points in the original coordinate frame. Let the components of the vector $\vec{y}_j$ contain the centered principal coordinates of quadrature point j, from Eq. (2.3), and $\vec{x}_j$ the desired full coordinates (uncentered) for this same point in the original frame. Then:

$$\vec{x}_j = \mathbf{G}\vec{y}_j + \vec{\mu}, \tag{2.4}$$

where the ith component of $\vec{\mu}$ gives the corresponding normalized first-order moment: $\vec{\mu}(i) = \langle m_i\rangle_f/N_0$. The quadrature weights (which sum to the total particle number density) are, of course, unchanged by the transformation: $w_j = 2^{-h}N_0$.

The steps for locating multivariate quadrature points from moments using the 2^h-quadrature point version of the PCA-QMOM are summarized as follows: (1) Set up the covariance matrix, Σ, consisting of the normalized moments of second order in the original coordinates, and solve the eigenvalue problem associated with this matrix to obtain the ordered principal values $\{\lambda_i\}$ and the matrix $\mathbf{G}$. (2) The location of the quadrature points in the principal frame is given immediately by Eq. (2.3). Convert these to the original coordinates using Eq. (2.4) and normalize to N_0. Eqs. (2.3) and (2.4) complete the assignment of quadrature points from moments in this version of the PCA-QMOM.

3. Moment evolution

The assignment of quadrature points from moments by the PCA-QMOM having been described, we complete closure by describing the method used to update the moments in terms of the quadrature points so assigned. The procedure is basically the same as in the original QMOM (McGraw, 1997; Barrett & Webb, 1998), but is extended here to the multivariate applications that are the focus of the present study. To illustrate, we consider below the mixed moments of (i) multicomponent aerosols evolving under coagulation and condensation, and (ii) mixed-shape single-component particles evolving under simultaneous coagulation and sintering. The same general methods apply to other kinds aerosol microphysical processes requiring a multivariate description; provided only that the rate kernels for these processes are known.

3.1. Multivariate condensation

Consider particle growth through the condensation/evaporation of condensable molecular species in a multicomponent vapor. The following equation gives the evolution of the mixed moment,

$\langle m_1^p m_2^q \cdots m_h^w \rangle_f$, for h component species under condensation:

$$\begin{aligned}\frac{\mathrm{d}}{\mathrm{d}t}\langle m_1^p m_2^q \cdots m_h^w \rangle_f &= \int \cdots \iint \frac{\mathrm{d}}{\mathrm{d}t}(m_1^p m_2^q \cdots m_h^w) f(m_1, m_2, \ldots, m_h)\,\mathrm{d}m_1\,\mathrm{d}m_2 \cdots \mathrm{d}m_h \\ &\approx \sum_{j=1}^{N} \frac{\mathrm{d}}{\mathrm{d}t}(m_{1j}^p m_{2j}^q \cdots m_{hj}^w) w_j. \end{aligned} \tag{3.1}$$

The first equality is derived in Appendix A of McGraw and Wright (2003) and the second gives the N-point quadrature approximation, using a single index j to number the points. Thus the coordinates $(m_{1j}, m_{2j}, \ldots, m_{hj})$ give the location of quadrature point j having weight w_j. Evaluation of the derivatives on the right-hand side requires the growth rate law for each component species (i). For example, the net addition (loss) of species i to (from) a particle having the composition $\{m_1, m_2, \ldots, m_h\}$ can be represented quite generally as

$$\frac{\mathrm{d}m_i}{\mathrm{d}t} = \phi_i(m_1, m_2, \ldots, m_h) \tag{3.2}$$

for $i = 1, 2, \ldots, h$. The right-hand side of Eq. (3.2) gives a net rate that depends on both condensation and evaporation fluxes, which in turn depend on the relative sizes of the particle and the mean free path of the gas, and particle composition. In some cases particle growth may to a good approximation depend only on radius, as with transport-limited growth, but in other cases, of high importance to atmospheric aerosols, composition-dependent thermodynamic models are necessary for improved prediction of evaporation rates and gas–particle exchange (Clegg, Brimblecombe, & Wexler, 1998; Capaldo, Pilinis, & Pandis, 2000). For these cases, the resulting growth laws take the more general multivariate form given by the right-hand side of Eq. (3.2) and their evaluation using thermodynamic models can become the most computationally expensive part of an aerosol simulation run. A great advantage of the PCA-QMOM is its property that the pdf is optimally represented by just a few quadrature points, so the number of evaluations of the right-hand side of Eq. (3.2) required during a simulation (one for each point) is minimized.

3.2. Multivariate coagulation

The moment evolution equations for coagulation are developed here for a trivariate (three component species) particle model to illustrate the method. The extension to higher dimensions is straightforward. Consider the coagulation of two three-component particles to form a single particle of larger size:

$$\{m_1, m_2, m_3\} + \{m_1', m_2', m_3'\} \Rightarrow \{m_1 + m_1', m_2 + m_2', m_3 + m_3'\}. \tag{3.3}$$

For this event the change in the moment $\langle m_1^p m_2^q m_3^w \rangle_f$ is

$$(m_1 + m_1')^p (m_2 + m_2')^q (m_3 + m_3')^w - m_1^p m_2^q m_3^w - m_{1'}^p m_{2'}^q m_{3'}^w. \tag{3.4}$$

Factoring in the frequency at which events of type (3.3) occur, which is proportional to the product of the distribution functions for each particle, and using Eq. (3.4), we obtain:

$$\begin{aligned}\frac{\mathrm{d}}{\mathrm{d}t}\langle m_1^p m_2^q m_3^w\rangle_f &= \frac{1}{2}\int\cdots\iint K(m,m')[(m_1+m_1')^p(m_2+m_2')^q(m_3+m_3')^w - m_1^p m_2^q m_3^w - m_{1'}^p m_{2'}^q m_{3'}^w] \\ &\quad\times f(m_1,m_2,m_3)f(m_1',m_2',m_3')\,\mathrm{d}m_1\,\mathrm{d}m_2\,\mathrm{d}m_3\,\mathrm{d}m_1'\,\mathrm{d}m_2'\,\mathrm{d}m_3'. \qquad (3.5)\end{aligned}$$

The factor 1/2 corrects for counting each pair of particles twice. In writing the kernel this way we have assumed that the coagulation rate depends only on the total masses of the two particles and not on their composition:

$$K(m,m') = K(m_1+m_2+m_3, m_1'+m_2'+m_3'). \qquad (3.6)$$

The quadrature approximation to Eq. (3.5) is:

$$\begin{aligned}\frac{\mathrm{d}}{\mathrm{d}t}\langle m_1^p m_2^q m_3^w\rangle_f \approx \frac{1}{2}\sum_j\sum_k K(m_j,m_k)[(m_{1j}+m_{1k})^p(m_{2j}+m_{2k})^q(m_{3j}+m_{3k})^w \\ - m_{1j}^p m_{2j}^q m_{3j}^w - m_{1k}^p m_{2k}^q m_{2k}^w]w_j w_k, \qquad (3.7)\end{aligned}$$

where the summation indices vary from 1 to the number of quadrature points, N. The coagulation kernel is often reported in terms of the particle volume $v(m_1, m_2, \ldots, m_c)$, which will in general have some dependence on the mixing state of the particle. For example, a homogeneous particle might well have a different volume than one of identical mass composition that is not homogeneously mixed. Here we assume that individual particles are spherical and homogeneously mixed, so expressing the coagulation kernel in terms of particle mass requires only an approximation for the particle density to determine the specific form of K. The method is also capable of handling more general kernels when their functional dependencies are known.

3.3. Simultaneous coagulation and sintering

Particles having identical composition but different shapes have been represented by assigning a volume, v, and surface area, a, to each particle (Koch & Friedlander, 1990). The v–a model has proven useful for the representation of particle aggregates undergoing simultaneous coagulation and sintering in flames (Wright, McGraw, & Rosner, 2001; Rosner & Pyykonen, 2002; Rosner, McGraw, & Tandon, 2003). Microphysical processes are represented through the dynamical equations developed for evolving the bivariate number density distribution function, $f(v,a)$, whose mixed moments are:

$$\langle v^p a^q\rangle_f = \iint v^p a^q f(v,a)\,\mathrm{d}v\,\mathrm{d}a. \qquad (3.8)$$

It is useful to summarize the moment evolution equations used in the v–a model (Wright et al., 2001) in preparation for the calculations of the following section. A coagulation event between

two particles, under the assumption that area as well as volume is additive, can be represented schematically as

$$\{v,a\}+\{v',a'\}\Rightarrow\{v+v',a+a'\}. \tag{3.9}$$

The change in the bivariate v–a moment $\langle v^k,a^l\rangle_f$ for this one event is

$$(v+v')^p(a+a')^q-v^pa^q-v'^pa'^q. \tag{3.10}$$

Integrating over the distribution, as in Eq. (3.5), gives

$$\begin{aligned}\left[\frac{\mathrm{d}}{\mathrm{d}t}\langle v^pa^q\rangle_f\right]_{\text{coag}}&=\frac{1}{2}\int\cdots\int\beta(v,v')[(v+v')^p(a+a')^q-v^pa^q-v'^pa'^q]\times f(v,a)f(v',a')\,\mathrm{d}v'\,\mathrm{d}a'\,\mathrm{d}v\,\mathrm{d}a\\&\approx\frac{1}{2}\sum_{j=1}^{N}\sum_{k=1}^{N}\beta(v_j,v_k)[(v_j+v_k)^p(a_j+a_k)^q-v_j^pa_j^q-v_k^pa_k^q]w_jw_k,\end{aligned} \tag{3.11}$$

where it has been assumed that the coagulation kernel, $\beta(v,v')$, depends only on volume.

For particles undergoing sintering, volume is conserved and (Wright et al., 2001):

$$\left[\frac{\mathrm{d}}{\mathrm{d}t}\langle v^pa^q\rangle_f\right]_{\text{fusion}}=q\iint v^pa^{q-1}\dot{a}f(v,a)\,\mathrm{d}v\,\mathrm{d}a\approx q\sum_{j=1}^{N}v_j^pa_j^{q-1}\dot{a}|_{a=a_j}w_j. \tag{3.12}$$

For the model calculations of the following section we use the linearized, surface-energy driven, rate law of Koch and Friedlander (1990), under which the time rate of change of surface area for an individual aggregate is

$$\dot{a}=-\frac{1}{t_f}(a-a_{\min}), \tag{3.13}$$

where $a_{\min}$ is the area of the fully compacted (spherical) particle of the same volume, and t_f is the characteristic time of fusion/sintering. Eqs. (3.11)–(3.13) complete the model.

3.4. Coordinate transformations and the evolution of transformed moments

It is sometimes more accurate to track moments and quadrature points in a transformed coordinate space. For example, aerosol distributions shaped by coagulation tend to be broad and transformation to $z=\ln(m)$ might be expected to better approximate a normal distribution (normal in z, lognormal in m) and better sampling of the pdf with the quadrature points assigned along z rather than along m. Calculations presented in the following section will employ transformations of the type $z_i=z_i(m_i)$ where $z_i(m_i)$ is the logarithm, as above, or a power law of the form: $z_i=m_i^{\gamma_i}$, with an exponent γ_i that will in general be coordinate dependent. Such coordinate transformations are easily carried out within the framework of the QMOM as next illustrated for selected transformations used in the calculations of the following section.

The covariance matrix and quadratures are cast in terms of the transformed moments. To illustrate for the bivariate case:

$$\langle z_1^p z_1^q \rangle = \iint z_1^p z_2^q f_z(z_1, z_2)\,\mathrm{d}z_1\,\mathrm{d}z_2 \approx \sum_j z_{1j}^p z_{2j}^q w_j. \tag{3.14}$$

Applying the fundamental transformation rule governing the mapping between coordinate systems: $f_z(z_1, z_2)\,\mathrm{d}z_1\,\mathrm{d}z_2 = f(m_1, m_2)\,\mathrm{d}m_1\,\mathrm{d}m_2$ greatly facilitates construction of the moment evolution equations in the transformed coordinates. For coagulation, Eq. (3.5) becomes:

$$\begin{aligned}\frac{\mathrm{d}}{\mathrm{d}t}\langle z_1^p z_2^q \rangle &= \frac{1}{2}\sum_{j=1}^{N}\sum_{k=1}^{N} K_z(z_{1j}, z_{2j}, z_{1k}, z_{2k})[z_1^p(m_{1j}+m_{1k}) z_2^q(m_{2j}+m_{2k}) - z_1^p(m_{1j}) z_2^q(m_{2j}) \\ &\quad - z_1^p(m_{1k}) z_2^q(m_{2k})] w_j w_k,\end{aligned} \tag{3.15}$$

where the transformed kernel is

$$K_z(z_{1j}, z_{2j}, z_{1k}, z_{2k}) = K(m_j, m_k) = K(z_{1j}^{1/\gamma_1} + z_{2j}^{1/\gamma_2}, z_{1k}^{1/\gamma_1} + z_{2k}^{1/\gamma_2})$$

for the power law transformation, and $K(\mathrm{e}^{z_{1j}} + \mathrm{e}^{z_{2j}}, \mathrm{e}^{z_{1k}} + \mathrm{e}^{z_{2k}})$ for the log.

For condensation, Eq. (3.1) becomes:

$$\frac{\mathrm{d}}{\mathrm{d}t}\langle z_1^p z_2^q \rangle = \iint \frac{\mathrm{d}}{\mathrm{d}t}(z_1^p z_2^q) f_z(z_1, z_2)\,\mathrm{d}z_1\,\mathrm{d}z_2 \approx \sum_{j=1}^{N} \frac{\mathrm{d}}{\mathrm{d}t}(z_{1j}^p z_{2j}^q) w_j. \tag{3.16}$$

The quadrature derivatives are evaluated using the chain rule and Eq. (3.2) for the growth law written in terms of two components for the bivariate case. Thus, for the power law transformations, $z_1 = m_1^{\gamma_1}$ and $z_2 = m_2^{\gamma_2}$, we obtain

$$\frac{\mathrm{d}z_{1j}}{\mathrm{d}t} = \frac{\mathrm{d}z_{1j}}{\mathrm{d}m_{1j}}\frac{\mathrm{d}m_{1j}}{\mathrm{d}t} = \gamma_1 z_{1j}^{(\gamma_1-1)/\gamma_1}\frac{\mathrm{d}m_{1j}}{\mathrm{d}t} = \gamma_1 z_{1j}^{(\gamma_1-1)/\gamma_1}\phi_1(z_{1j}^{1/\gamma_1}, z_{2j}^{1/\gamma_2}) \tag{3.17a}$$

and for the log transformation

$$\frac{\mathrm{d}z_{1j}}{\mathrm{d}t} = \frac{\mathrm{d}z_{1j}}{\mathrm{d}m_{1j}}\frac{\mathrm{d}m_{1j}}{\mathrm{d}t} = \exp(-z_{1j})\frac{\mathrm{d}m_{1j}}{\mathrm{d}t} = \exp(-z_{1j})\phi_1[\exp(z_{1j}), \exp(z_{2j})]. \tag{3.17b}$$

Finally, for evolution of the transformed bivariate v–a moments under sintering: With $z_1 = v^{\gamma_1}$ and $z_2 = a^{\gamma_2}$, Eq. (3.12) becomes

$$\left[\frac{\mathrm{d}}{\mathrm{d}t}\langle z_1^p z_2^q \rangle\right]_{\text{fusion}} = \iint z_1^p \frac{\mathrm{d}z_2^q}{\mathrm{d}t} f(z_1, z_2)\,\mathrm{d}z_1\,\mathrm{d}z_2 \approx \gamma_2 q \sum_{j=1}^{N} z_{1j}^p z_{2j}^{q-1} z_{2j}^{(\gamma_2-1)/\gamma_2} \dot{a}|_{a=(z_{2j})^{1/\gamma_2}} w_j. \tag{3.18}$$

The preceding power law transformations are fully consistent with Eqs. (3.1), (3.7), and (3.12) applied to the corresponding fractional moments. Thus one can change easily from integral moments to fractional moments such as $v^{p/3}$ or $a^{q/2}$ which, in this example, are proportional to the radial

moments for integer values of p and q. The log transformation is well suited to broad pdfs that resemble log-normal form. On the other hand, for certain analytic coagulation kernels, such as $K(u,v)=\text{const}$, $K(u,v)=u+v$, and $K(u,v)=uv$, where u and v are particle volumes, the QMOM is exact for the integral volume moments, but only approximate for the moments of $\log(v)$ and fractional volume moments. Nevertheless, the QMOM remains highly accurate for transformed moments, as shown recently in comparisons with the moments obtained from box model simulations of the full pdf using high-resolution discrete models (McGraw & Wright, 2003).

4. Calculations

4.1. Simultaneous coagulation and sintering in the bivariate v–a model

Simulation of the full bivariate pdf in the volume–area (v–a) model of Section 3.3 was recently reported (Wright et al., 2001). The pdf was evolved on a 150×150 discrete v–a grid, and selected mixed moments were evaluated numerically as a function of time by summing over the grid. These results will be used here to benchmark the PCA-QMOM for a nonanalytic case.

Fig. 1a shows evolution of the fractional volume moments, $\{\langle 1\rangle, \langle v^{1/3}\rangle, \langle v^{2/3}\rangle, \langle v\rangle, \langle v^{4/3}\rangle, \langle v^{5/3}\rangle\}$, and Fig. 1b the mixed moments, $\{\langle v^0 a^{5/3}\rangle, \langle v^{1/3}a^{5/3}\rangle, \langle v^{2/3}a^{5/3}\rangle, \langle v a^{5/3}\rangle, \langle v^{4/3}a^{5/3}\rangle, \langle v^{5/3}a^{5/3}\rangle\}$, defined as in Eq. (3.8). The discrete grid calculations are as in Wright et al. (2001). The coagulation kernel was approximated as

$$\beta(v_j, v_k) = K(v_j^{-1/3} + v_k^{-1/3})(v_j^{1/3} + v_k^{1/3}), \tag{4.1}$$

which applies for Brownian coagulation in the continuum regime. The constraint $a \geqslant a_{\min}(v)$, where $a_{\min}(v)$ is the minimum surface area for a particle of volume v, is handled by building it into the grid itself as described in Wright et al. (2001). The initial distribution is lognormal in these modified volume and area coordinates. Time is expressed in reduced units, $\tau = KN(0)t$, where K is the coagulation rate constant from Eq. (4.1) (assumed independent of time) and $N(0)$ is the initial number of particles per unit volume (initial value of $\langle v^0 a^0\rangle \equiv \langle 1\rangle$ from Eq. (3.8)).

Fig. 2a shows a sampling of 1000 points from the initial distribution. Quadrature points were assigned by the PCA-QMOM after first transforming coordinates so that the initial distribution optimally approximates a bivariate normal form. Results from the Box–Cox transformation (Appendix A) suggest a power law transformation with $z_1 = v^{1/10}$ and $z_2 = a^{-1/10}$ for the volume and area coordinates, respectively. That these exponents are small in magnitude is consistent with an initial distribution nearly lognormal in v and a (Appendix A). The sampled points from Fig. 2a are reproduced in Fig. 2b in the transformed coordinates, and the quadrature points assigned in these coordinates using PCA (Section 2). Fig. 2b shows orientation of the principal axes, y_1 and y_2, and initial placement of the four quadrature points obtained from the six transformed-coordinate moments $\{\langle 1\rangle, \langle z_1\rangle, \langle z_2\rangle, \langle z_1^2\rangle, \langle z_2^2\rangle, \langle z_1 z_2\rangle\}$. These give the normalization, the two coordinate means, and the three distinct elements of the symmetric 2×2 covariance matrix, respectively. Fig. 2b also shows the initial disposition of the probability ellipsoids for the σ (1 standard deviation) and 2σ (2 standard deviation) surfaces obtained from the covariance matrix as described in Paper I. The four quadrature points, rectilinear in the coordinates of Fig. 2b, are shown after transformation back to

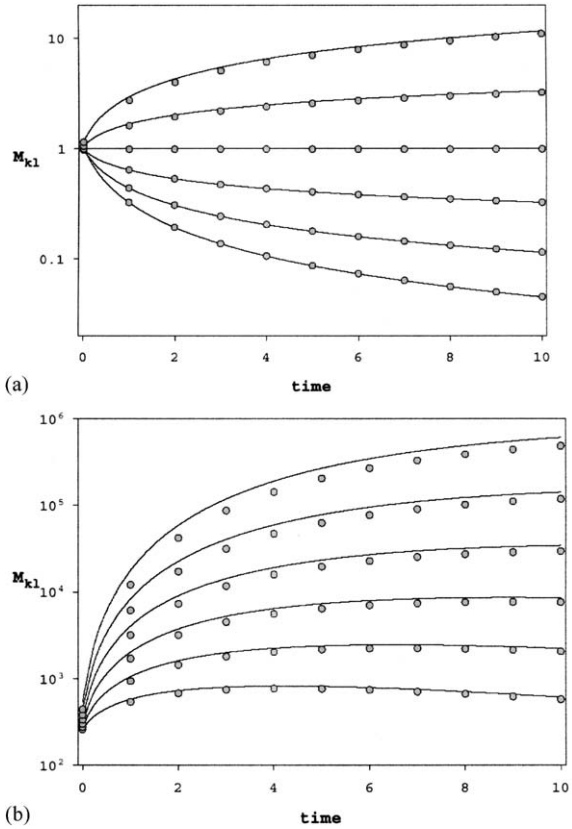

Fig. 1. (a) Evolution of the volume moments ($p = 0, 1/3, 2/3, 1, 4/3, 5/3$; $q = 0$, in Eq. (3.8)). (b) Evolution of the mixed moments ($p = 0, 1/3, 2/3, 1, 4/3, 5/3$; $q = 5/3$, in Eq. (3.8)). The exponent p increases from the lowest to highest curves shown in each panel. Curves: reference results from numerical calculations using a 150×150 discrete grid model (from Wright et al., 2001). Points, shown at integral values of the reduced time (see text), are the PCA-QMOM results obtained by tracking four equal weight quadrature points.

the original v–a coordinates in Fig. 2a. These have equal weights (irrespective of coordinates) and are seen to provide an excellent economical representation of the initial distribution.

Returning to Fig. 1, the data points, shown at integral values of the reduced time, were calculated using this four-point quadrature version of the PCA-QMOM. Moments were evolved using the differential equations for coagulation and sintering given by the coordinate transformed versions of Eqs. (3.11) and (3.12), respectively (Section 3.4). The PCA-QMOM results are seen to be in excellent agreement with the benchmark calculations for the lower-order moments (Fig. 1a and lower curves of Fig. 1b), with the largest error, approaching 20%, encountered for the highest order moment (upper curve of Fig. 1b). The systematically lower results from the PCA-QMOM seen for the higher moments in Fig. 1b is likely due to failure to capture the tail of the distribution, which has its greatest influence on the higher-order moments, using just three moments/two quadrature points per variable. For comparison, the bivariate QMOM of Wright et al. (2001) gave errors within 1% using a 12-point quadrature technique (with the quadrature abscissas and weights determined

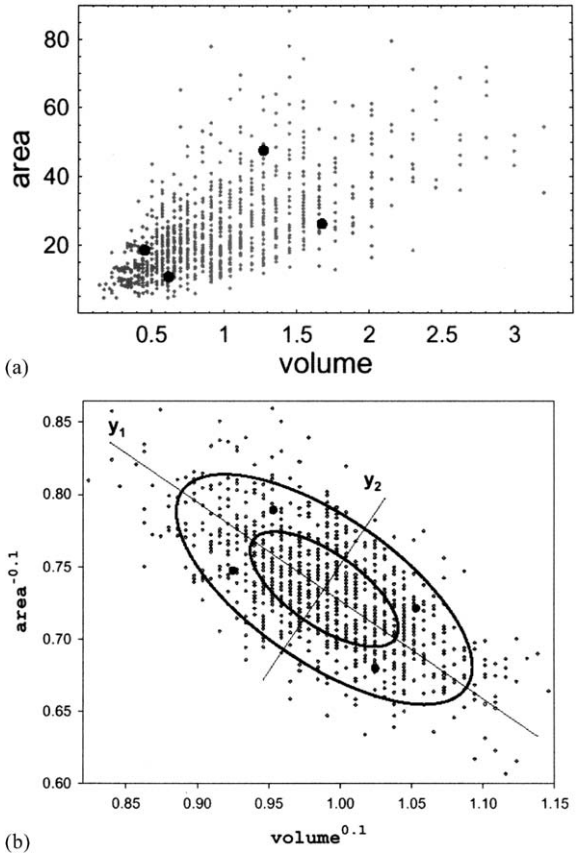

Fig. 2. (a) Sampled bivariate distribution (1000 points) in volume and area coordinates. Initial location of the four quadrature points obtained from the PCA-QMOM after coordinate transformation is also shown. (b) Sample points after coordinate transformation. Initial locations of the principal axes, four quadrature points, and σ and 2σ elliptical surfaces from the PCA-QMOM are also shown.

using 36 bivariate moments), and within 7% for a multiple three-point quadrature technique (four sets of three-point quadratures) also using 36 bivariate moments. The accuracy of the four-point (six moment) PCA-QMOM is comparable to that of a single three-point (nine moment) quadrature using the original bivariate QMOM.

4.2. Interacting particle populations

There are important cases where the aerosol pdf is not well approximated by a single multivariate normal pdf in any coordinate system. Examples include external mixtures of distinct particle populations as may be found near sources of primary emissions. While not mixed initially, such populations can subsequently interact through coagulation, and also through condensation via the competition for limited condensable vapor species. Recent studies have pointed to the mixing state of the aerosol as important in climate and health effects, and one would like to have the capability to simulate

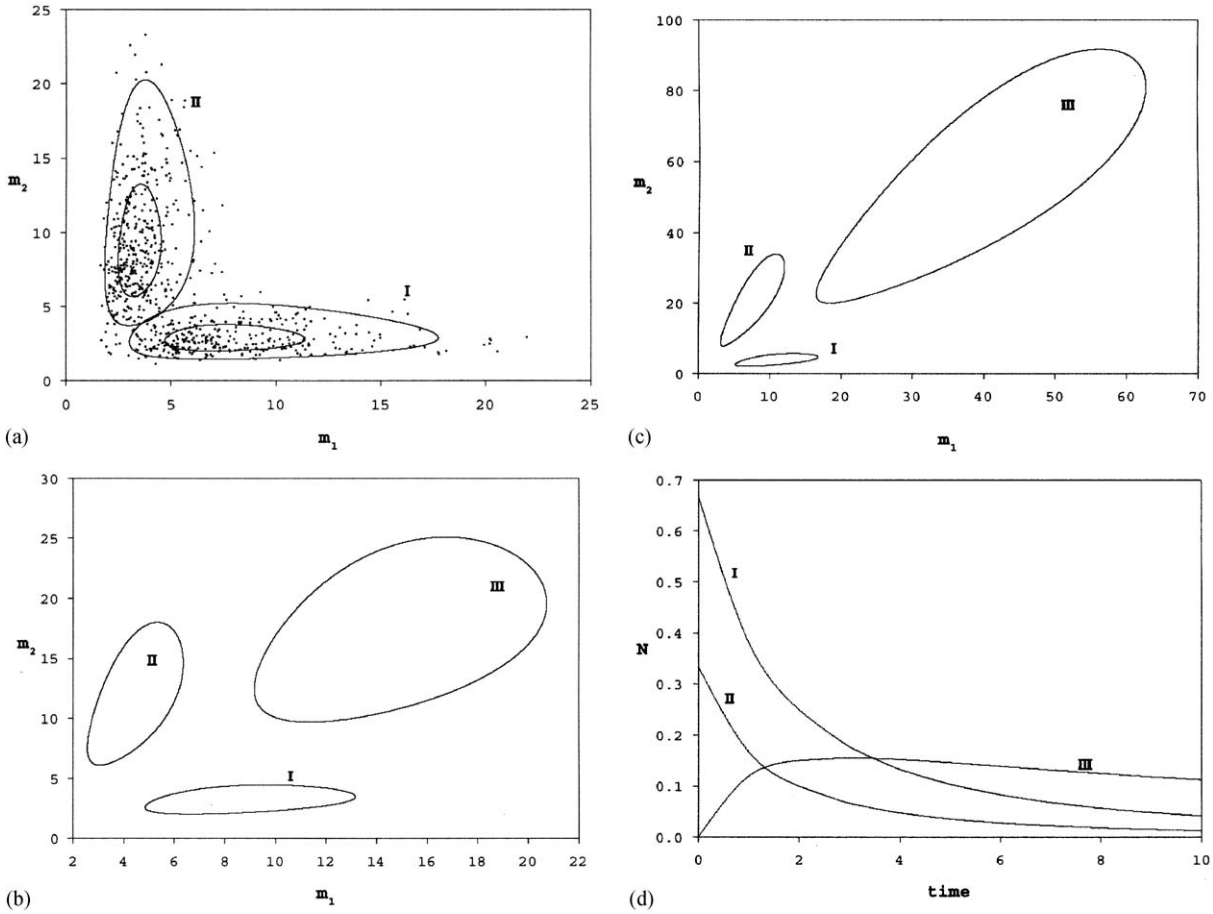

Fig. 3. Simulation of interacting particle populations. (a) Initial condition. Sampled distributions and σ and 2σ surfaces in species mass coordinates. These surfaces are elliptical in the log-mass coordinates employed in the simulation. (b) and (c) σ surfaces at reduced coagulation times $t_{\text{coag}} = 5$ and $t_{\text{coag}} = 10$, respectively. The mixed population, III, consists of aggregates formed via coagulation of particles from either I, II, or III with the other populations. (d) Number density of particles in each distribution as a function of reduced time. The initial total particle number density is normalized to unity.

the general mixing state of a multivariate aerosol throughout its evolution. The great computational efficiency of moment methods allows these kinds of problems to be handled with comparative ease through the simultaneous tracking of multiple distributions. The following calculation illustrates how the PCA-QMOM can be applied to the simulation of interacting particle populations.

Fig. 3a shows the initial condition for the test calculation. The aerosol is represented as a sum of two, initially known, bivariate lognormal distributions (I and II), with moments:

$$\{\langle 1\rangle_{\text{I}} = N_1; \langle z_1\rangle_{\text{I}} = 2; \langle z_2\rangle_{\text{I}} = 1; \langle z_1^2\rangle_{\text{I}} = 0.2; \langle z_2^2\rangle_{\text{I}} = 0.1; \langle z_1 z_2\rangle_{\text{I}} = 0.01\}, \tag{4.2a}$$

$$\{\langle 1\rangle_{\text{II}} = N_2; \langle z_1\rangle_{\text{II}} = 1.2; \langle z_2\rangle_{\text{II}} = 2.2; \langle z_1^2\rangle_{\text{II}} = 0.1; \langle z_2^2\rangle_{\text{II}} = 0.2; \langle z_1 z_2\rangle_{\text{II}} = 0.01\}. \tag{4.2b}$$

The σ and 2σ surfaces and sampled particle compositions from the initial distributions are shown in the figure. These surfaces are elliptical in the logarithmic coordinate system, $z_1 = \ln(m_1)$, $z_2 = \ln(m_2)$, used in the simulation. Interactions take place through coagulation both within and between the different populations. In the latter case we define a third, mixed, population (III) that gains through the assignment to it of aggregates formed via coagulation of particles from either I or II with the other populations. The pdf of the overall particle population is represented as a sum of contributions from the component distributions: $f(m_1, m_2) = f_{\mathrm{I}}(m_1, m_2) + f_{\mathrm{II}}(m_1, m_2) + f_{\mathrm{III}}(m_1, m_2)$. Separately assigned quadrature points and moments can be tracked for each of these distributions as well as for the overall population. Extension of Eq. (3.3) to this case gives, now for two components, the following representative processes:

$$\begin{aligned}
&\{m_1, m_2\}_{\mathrm{I}} + \{m_1', m_2'\}_{\mathrm{I}} \Rightarrow \{m_1 + m_1', m_2 + m_2'\}_{\mathrm{I}},\\
&\{m_1, m_2\}_{\mathrm{I}} + \{m_1', m_2'\}_{\mathrm{II}} \Rightarrow \{m_1 + m_1', m_2 + m_2'\}_{\mathrm{III}},\\
&\{m_1, m_2\}_{\mathrm{I}} + \{m_1', m_2'\}_{\mathrm{III}} \Rightarrow \{m_1 + m_1', m_2 + m_2'\}_{\mathrm{III}}
\end{aligned} \tag{4.3}$$

and similarly for other allowable combinations.

For special kernels [which include the constant kernel, $K(m, m') = K$; the sum kernel, $K(m, m') = m + m'$; the product kernel $K(m, m') = mm'$; and their linear combinations] the moment evolution equations in mass coordinates can be expressed in closed form and moment methods including the QMOM and PCA-QMOM are exact. This property extends even to the case of multiply interacting populations. For the total distribution, $f(m_1, m_2)$, to illustrate for the constant kernel case, the evolution equations for moments through second order are:

$$\begin{aligned}
&\frac{\mathrm{d}N}{\mathrm{d}t} = -\frac{K}{2} N^2,\\
&\frac{\mathrm{d}\langle m_a \rangle}{\mathrm{d}t} = 0,\\
&\frac{\mathrm{d}\langle m_a^2 \rangle}{\mathrm{d}t} = K \langle m_a \rangle^2,\\
&\frac{\mathrm{d}\langle m_a m_b \rangle}{\mathrm{d}t} = K \langle m_a \rangle \langle m_b \rangle,
\end{aligned} \tag{4.4}$$

where a and b label different species. This closed set of equations determines all of the moments required by the simplest (2 points per coordinate) version of the PCA-QMOM. Multiple populations are tracked using separate covariance matrices for each population. For three populations and two components, a total of 18 moments is required. These generate three sets of four-point quadratures; one set for each distribution. For simulations in mass coordinates using analytic kernels, this full set of moment evolution equations is closed and the PCA-QMOM is exact.

Figs. 3b and 3c show evolved σ surfaces for each of the populations at the reduced coagulation times $t_{\mathrm{coag}} = 5$ and 10 defined below. These results were obtained from a PCA-QMOM simulation carried out in the log-mass coordinate frame using Eq. (3.15) with constant K. Except for particle number, moment evolution in the transformed coordinates is no longer exact. Nonetheless, the use

of transformed-coordinate quadratures often provides superior sampling of pdf shape (as is evident for the near lognormal distribution of Fig. 2), and better approximations to integrals over kernels describing aerosol physical and optical properties, than if the analytic mass coordinates are used. Fig. 3d shows the number of particles remaining in each distribution as a function of reduced time. These results are independent of the total number concentration of particles initially present (shown normalized to unity). Particle number enters the reduced coagulation time, defined as $t_{\mathrm{coag}}=K[N_{\mathrm{I}}(0)+N_{\mathrm{II}}(0)]t=KN(0)t$. The figure shows decay of the initial populations (I and II) and growth, and later decay, of the mixed population (III).

4.3. Evolution of generally mixed multicomponent aerosols

Calculations were completed for a number of test cases involving multicomponent aerosols evolving under condensation and coagulation to test the general numerical integration features of the PCA-QMOM in higher coordinate dimensions. Again we find for those special cases that closed-form equations can be constructed for the moments, the PCA-QMOM integration is also exact. The presentation will be limited mainly to results obtained for coagulation, as this is the most interesting case.

Fig. 4 shows evolution of a three-component aerosol in logarithmic mass coordinates. The initial distribution is taken to be a product of lognormal distributions with identical distribution parameters for each component:

$$f_i(m_i,0)/N_0=(m_i s_i\sqrt{2\pi})^{-1}\exp\{-[\ln(m_i/\overline{m_i})]^2/(2s_i^2)\}\}, \tag{4.5a}$$

where m_i is the mass of species i in the particle, $\overline{m_i}$ is the geometric mean mass, and s_i is the logarithm of the geometric standard deviation. Here we set $s_1=s_2=s_3\equiv s$ and $\overline{m_1}=\overline{m_2}=\overline{m_3}\equiv\bar{m}$. The initial distribution takes the factorable form:

$$f(m_1,m_2,m_3;0)=N_0[m_1m_2m_3(s\sqrt{2\pi})^3]^{-1}\exp\left\{-\sum_{i=1}^{3}[\ln(m_i/\bar{m})]^2/(2s^2)\}\right\} \tag{4.5b}$$

with initial moments:

$$\langle m_1^p m_2^q m_3^w;0\rangle_f=N_0\exp\{p\bar{m}+(ps)^2/2\}\exp\{q\bar{m}+(qs)^2/2\}\exp\{w\bar{m}+(ws)^2/2\}. \tag{4.6}$$

Fig. 4a shows a sampling of the initial distribution (small black points) and the initial σ and 2σ probability surfaces, colored blue and green respectively, for $s^2=\ln(4/3)$ and $\bar{m}=\sqrt{3}/2$. These initial distribution surfaces are spherical in logarithmic coordinates. The 2^h-point PCA-QMOM yields eight equal weight quadrature points, initially at the vertices of the cube, indicated by the red points. (Note that, because of the initial spherical symmetry of the pdf, there is a degeneracy here in the initial assignment of quadrature points. This is irrelevant for computation as the moments and σ-surfaces evolve continuously—and the spherical pdf symmetry is broken immediately once the particles begin to interact.) The test distribution is evolved under simultaneous coagulation (constant

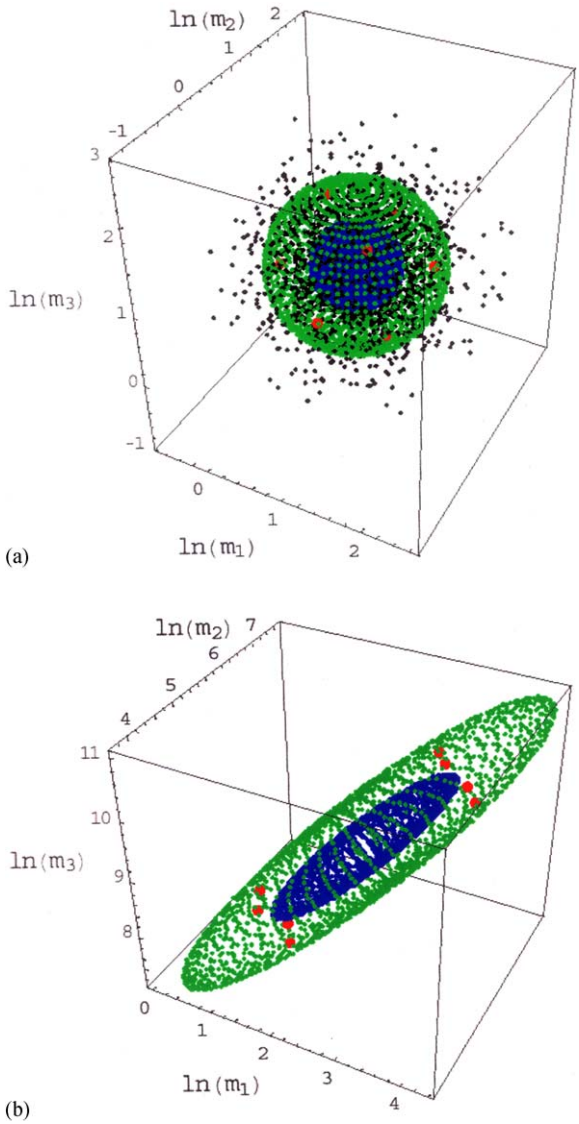

Fig. 4. Evolution of a three-component aerosol in logarithmic mass coordinates under simultaneous coagulation and condensation. (a) σ (blue) and 2σ (green) surfaces and sampled compositions for the initial trivariate distribution given by Eq. (4.5b). (b) σ (blue) and 2σ (green) surfaces at reduced time (see text) $\tau = t_{\text{cond}} = t_{\text{coag}} = 10$. The red points in (a) and (b) are the eight equal-weight quadrature points tracked in the PCA-QMOM at $\tau = 0$ and 10, respectively. Elongation of the ellipsoidal surfaces at $\tau = 10$ reflects the emergence of a dominant principal coordinate (particle mass) during the approach to internal mixing.

kernel) and condensation growth. The condensation rate is taken to have the simple analytic form:

$$\frac{\mathrm{d}m_1}{\mathrm{d}t} = 0, \quad \frac{\mathrm{d}m_2}{\mathrm{d}t} = \frac{C}{3}\, m_2, \quad \frac{\mathrm{d}m_3}{\mathrm{d}t} = \frac{2C}{3}\, m_3, \tag{4.7}$$

where C is constant. The coagulation-to-condensation time constant ratio is set to unity: $\chi = KN(0)/C = 1$, to obtain comparable time scales for these processes. Results are given in terms of the reduced condensation time $t_{\text{cond}} = Ct$, which for this case ($\chi = 1$) equals the reduced coagulation time, t_{coag}. The PCA-QMOM is applied in logarithmic coordinates; evolving the moments according to Eqs. (3.16) and (3.17b) for condensation, and Eq. (3.15) for coagulation. Disposition of the eight quadrature points and the σ and 2σ surfaces is shown in Fig. 4b for $\tau = t_{\text{cond}} = t_{\text{coag}} = 10$. The figure shows the initial stages of approach to an internal mixing state for which total particle mass, the leading principal coordinate, becomes increasingly dominant while the orthogonal coordinates become diminished in importance, having significantly smaller variances in the principal frame. Such reductions in dimensionality are well captured by the PCA-QMOM. This effect is next examined more closely for a multicomponent aerosol evolving under coagulation alone.

Statistical features of the PCA-QMOM, including data compression, may be demonstrated through analytic solutions for the covariance matrix, $\Sigma(t)$, available when analytic growth laws are used. Eqs. (4.4), for constant-kernel coagulation, apply to any number of aerosol component species (coordinates) represented by the subscripts a and b. For h species, a and b will each vary from 1 through h. With the time dependence of the covariance matrix elements given by Eqs. (4.4) the matrix can be integrated directly to obtain:

$$\Sigma(t) = \Sigma(0) + K\mathbf{A}t. \tag{4.8}$$

$\mathbf{A}$ is the matrix of derivatives, constant in time, from the right-hand side of Eq. (4.4):

$$\mathbf{A} = \begin{pmatrix} \langle m_1\rangle^2 & \langle m_1\rangle\langle m_2\rangle & \cdots & \langle m_1\rangle\langle m_h\rangle \\ \langle m_1\rangle\langle m_2\rangle & \langle m_2\rangle^2 & \cdots & \langle m_2\rangle\langle m_h\rangle \\ \vdots & \vdots & & \vdots \\ \langle m_1\rangle\langle m_h\rangle & \langle m_2\rangle\langle m_h\rangle & \cdots & \langle m_h\rangle^2 \end{pmatrix} = \begin{pmatrix} \langle m_1\rangle \\ \langle m_2\rangle \\ \vdots \\ \langle m_h\rangle \end{pmatrix} \begin{pmatrix} \langle m_1\rangle & \langle m_2\rangle & \cdots & \langle m_h\rangle \end{pmatrix}. \tag{4.9}$$

The second equality shows $\mathbf{A}$ written as the outer product of the vector of component masses, $\mathbf{v}_1 = (\langle m_1\rangle\ \langle m_2\rangle\ \cdots\ \langle m_h\rangle)^{\mathrm{T}}$, with itself. Determined by a single vector, it follows that $\mathbf{A}$ has rank 1 and $h-1$ of its eigenvalues are equal to zero. The eigenvector of nonzero eigenvalue is obtained simply by multiplying Eq. (4.9) on the right-hand side by $\mathbf{v}_1$ to give

$$\mathbf{A}\begin{pmatrix} \langle m_1\rangle \\ \langle m_2\rangle \\ \vdots \\ \langle m_h\rangle \end{pmatrix} = \begin{pmatrix} \langle m_1\rangle \\ \langle m_2\rangle \\ \vdots \\ \langle m_h\rangle \end{pmatrix} \begin{pmatrix} \langle m_1\rangle & \langle m_2\rangle & \cdots & \langle m_h\rangle \end{pmatrix} \begin{pmatrix} \langle m_1\rangle \\ \langle m_2\rangle \\ \vdots \\ \langle m_h\rangle \end{pmatrix} = \sum_{i=1}^{h} \langle m_i\rangle^2 \begin{pmatrix} \langle m_1\rangle \\ \langle m_2\rangle \\ \vdots \\ \langle m_h\rangle \end{pmatrix} \tag{4.10}$$

showing that $\mathbf{v}_1$ is the eigenvector (unnormalized) of $\mathbf{A}$:

$$\mathbf{A}\mathbf{v}_1 = (\mathbf{v}_1 \cdot \mathbf{v}_1^{\mathrm{T}})\mathbf{v}_1 = \lambda_1\mathbf{v}_1 \tag{4.11a}$$

with nonzero eigenvalue

$$\lambda_1 = \langle m_1 \rangle^2 + \langle m_2 \rangle^2 + \cdots + \langle m_h \rangle^2. \tag{4.11b}$$

At long time the covariance matrix approaches $K\mathbf{A}t$ (see Eq. (4.8)) and its nonzero principal value is given by Eq. (4.11b). Inspection of the corresponding eigenvector, $\mathbf{v}_1$, shows that the principal axes is oriented along the coordinate direction, having constant component mass ratios $m_2/m_1 = \langle m_2 \rangle / \langle m_1 \rangle$, etc. This is the coordinate describing the internally mixed state of the aerosol, as expected on physical grounds.

4.4. Scaling of multicomponent aerosol distributions under coagulation

The long time asymptotic behavior of an evolving aerosol can also be studied using the PCA-QMOM. For this it is convenient to use nondimensional moments and scaled coordinates for the multivariate particle distribution function. Nondimensional moments are defined as

$$\langle \eta_1^j \eta_2^k \ldots \eta_h^l \rangle_\psi = \iiint \eta_1^j \eta_2^k \ldots \eta_h^l \psi(\eta_1, \eta_2, \ldots, \eta_h)\, \mathrm{d}\eta_1\, \mathrm{d}\eta_2 \ldots \mathrm{d}\eta_h, \tag{4.12}$$

where $\eta_a = m_a/\bar{m}_a$, etc. are scaled coordinates, $\bar{m}_a = \langle m_a \rangle / N$, and $\psi(\cdot)$ is the normalized, transformed version of $f(\cdot)$. The nondimensional moments are readily expressed in terms of the mass moments:

$$\langle \eta_1^j \eta_2^k \ldots \eta_h^l \rangle_\psi = \frac{\langle m_1^j m_2^k \ldots m_h^l \rangle_f}{N} \left(\frac{N}{\langle m_1 \rangle} \right)^j \left(\frac{N}{\langle m_2 \rangle} \right)^k \times \cdots \times \left(\frac{N}{\langle m_h \rangle} \right)^l. \tag{4.13}$$

Thus:

$$\langle 1 \rangle_\psi = \langle 1 \rangle_f / N = 1, \tag{4.14a}$$

$$\langle \eta_a \rangle = 1, \tag{4.14b}$$

$$\langle \eta_a^2 \rangle = \frac{\langle m_a^2 \rangle}{N} \left(\frac{N}{\langle m_a \rangle} \right)^2 = N \frac{\langle m_a^2 \rangle}{\langle m_a \rangle^2}, \tag{4.14c}$$

$$\langle \eta_a \eta_b \rangle = \frac{\langle m_a m_b \rangle}{N} \frac{N}{\langle m_a \rangle} \frac{N}{\langle m_b \rangle} = N \frac{\langle m_a m_b \rangle}{\langle m_a \rangle \langle m_b \rangle}. \tag{4.14d}$$

The reduced covariance matrix, corresponding to the reduced mass probability distribution $\psi(\eta_1, \eta_2)$, is:

$$\tilde{\Sigma}(t) = \begin{pmatrix} \langle \eta_1^2 \rangle - 1 & \langle \eta_1 \eta_2 \rangle - 1 & \cdots & \langle \eta_1 \eta_h \rangle - 1 \\ \langle \eta_1 \eta_2 \rangle - 1 & \langle \eta_2^2 \rangle - 1 & \cdots & \langle \eta_2 \eta_h \rangle - 1 \\ \vdots & \vdots & & \vdots \\ \langle \eta_1 \eta_h \rangle - 1 & \langle \eta_2 \eta_h \rangle - 1 & \cdots & \langle \eta_h^2 \rangle - 1 \end{pmatrix}. \tag{4.15}$$

The matrix elements of Eq. 4.15 are related to the elements of the original covariance matrix through **A** of Eq. 4.9:

$$\Sigma_{ij}(t) = \frac{\mathbf{A}_{ij}}{N(t)}\,\tilde{\Sigma}_{ij}(t) + \frac{\mathbf{A}_{ij}}{N(t)} - \mathbf{A}_{ij}. \tag{4.16}$$

For constant kernel:

$$\Sigma_{ij}(t) = \Sigma_{ij}(0) + K\mathbf{A}_{ij}t,$$
$$\tilde{\Sigma}_{ij}(t) + 1 = \left(\tilde{\Sigma}_{ij}(0) + 1\right)\frac{N}{N_0} + KNt \tag{4.17}$$

from Eq. (4.8), where $N_0 = N(0)$ is the initial particle number density. The first of Eqs. (4.4) gives the solution for N:

$$N(t) = \left(\frac{1}{N_0} + \frac{K}{2}t\right)^{-1} \tag{4.18}$$

and the second of Eqs. (4.17) gives the evolution of the reduced covariance matrix:

$$\tilde{\Sigma}(t) = \left(1 + \frac{KN_0t}{2}\right)^{-1}\left[\tilde{\Sigma}(0) + \mathbf{U} + KN_0\mathbf{U}t\right] - \mathbf{U}, \tag{4.19}$$

where **U** is the constant element $h \times h$ matrix having each of its elements equal to unity. In reduced time units, $t_{\text{coag}} = KN_0t$, this becomes:

$$\tilde{\Sigma}(t_{\text{coag}}) = \left(1 + \frac{t_{\text{coag}}}{2}\right)^{-1}\left[\tilde{\Sigma}(0) + \mathbf{U} + \mathbf{U}t_{\text{coag}}\right] - \mathbf{U}. \tag{4.20}$$

Fig. 5 shows evolution from an initial distribution (sampled points) towards the self-preserving limit for coagulation of a two component aerosol under constant kernel. The figure shows disposition of the four quadrature points for several indicated values of the reduced time. These lie at the vertices of rectangles into which can be inscribed the σ-surfaces (not shown) derived from the covariance matrix of Eq. (4.20). The corners of the small rectangle, oriented with the sampled points, mark the locations of the initial quadrature points. Subsequent locations are marked by clockwise rotation and lengthening of the principal axes with time. At long times the total mass coordinate dominates, and the distribution approaches a self-preserving form in the reduced total mass, $\eta \equiv m/\bar{m}$. The η-moments are known to approach, in the asymptotic limit, the factorial values $\langle \eta^k \rangle = \Gamma(k+1)$ under constant-kernel coagulation (Wang, 1966). Inspection of the long-time behavior of Fig. 5 shows merging of pairs of quadrature points to η values of 0 and 2 with combined weights of 1/2 for each merged pair (since each of the merging points has weight 1/4). These quadrature fixed points yield asymptotic moments in agreement with the factorial values for $k = 0, 1, 2$, showing that the PCA-QMOM gives the correct asymptotic behavior for this important analytic test case. These results illustrate the compression features of the PCA-QMOM. Compression is obtained with the dominance of a few principal coordinates (here just one) from the h originally required to specify the pdf. This reduction in dimensionality is especially important when the original dimensionality is large ($h \gg 1$).

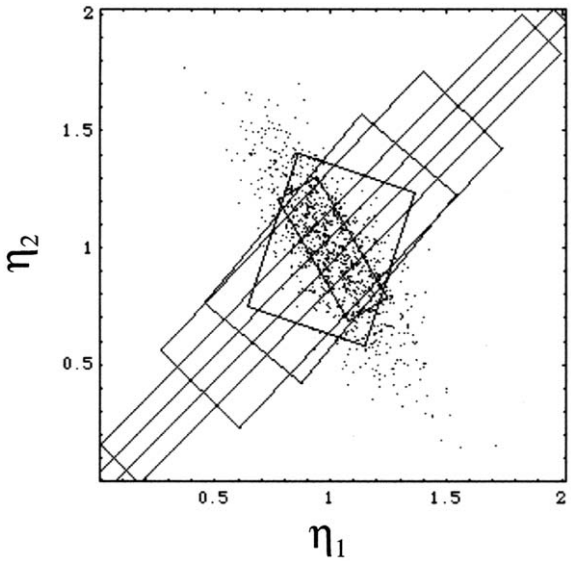

Fig. 5. Evolution from an initial distribution (sampled points) towards the self-preserving limit for coagulation of a two-component aerosol. Results are in scaled coordinates (mass divided by averaged mass). The figure depicts evolution of four equal-weight quadrature points from the PCA-QMOM. These are located at the corners of the six rectangles corresponding to reduced coagulation times of $t_{\text{coag}} = 0, 0.1, 0.3, 1.0, 10.0$, and 100.0. Subsequent locations are marked by clockwise rotation and lengthening of the principal axes with time. At long times the total mass coordinate dominates, and the pdf approaches a self-preserving, internally mixed, distribution in the reduced total mass $\eta = m/\bar{m}$.

5. Summary and discussion

The PCA-QMOM introduced in Paper I has been applied to the simulation of generally mixed, multivariate particle populations evolving under condensation, coagulation, and simultaneous condensation/coagulation and coagulation/sintering processes. The new method was tested through comparisons with the bivariate pdf obtained numerically using a high-resolution discrete grid model, and with analytic test cases in three and higher dimensions, where calculations of the full multivariate pdf are too expensive, computationally, to carry out.

The statistically based PCA-QMOM, which like all QMOM-based methods works best with lower-order moments, is in many ways complementary to the sectional and discrete grid approaches that seek to represent the full pdf. For univariate problems, QMOM calculations have typically employed three quadrature points (six moments). Although the QMOM has been shown to be remarkably accurate at this level (Marchisio, Pikturna, Fox, Vigil, & Barresi, 2003; McGraw & Wright, 2003), one may still seek (at least in the univariate case) more information by computing the full pdf using a high-resolution sectional model. On the other hand, for bivariate and especially for multivariate problems, it becomes vastly more difficult, even impractical, to track the full pdf, and statistical approaches will likely win out. Beyond the advantages of data compression available with PCA, there are many more lower-order (mixed) moments available in higher dimensions—and correspondingly higher densities of quadrature points can be assigned and tracked with time using the

methods we have described. Thus, much more information about a multivariate pdf, albeit of a statistical nature, becomes available with the PCA-QMOM.

Note added: An anonymous reviewer raises the interesting question as to how the PCA-QMOM incorporates a constraint such as a charge balance. To illustrate, consider a neutral particle containing the three ionic species H^+, NH_4^+, and SO_4^{2-}. The presence of neutral species such as water will give rise to additional particle coordinates, but for purpose of illustration we limit discussion to just these three. Let $x_1 = n(H^+)$, $x_2 = n(NH_4^+)$, and $x_3 = n(SO_4^{2-})$ be the number of ions of each type in the particle. Charge neutrality requires $x_1 + x_2 - 2x_3 = 0$, defining a plane in the three dimensional coordinate space defined by x_1, x_2, and x_3. For an initial distribution satisfying neutrality, it is readily shown that the leading principal axis y_1 and y_2 will automatically lie in the plane defined by the neutrality condition while the third coordinate, y_3, will have zero variance ($\lambda_3 = 0$) and zero mean. It is then up to the particle growth laws to maintain charge balance if the neutrality condition is to be preserved. For particle growth laws that maintain charge balance, the distribution will, ideally, continue to evolve in the neutrality plane. More generally, y_3 is proportional to particle charge and nonzero values for its mean, $\langle y_3 \rangle$, or variance, λ_3, provide quantitative measures of any failure to satisfy the neutrality condition. In general, if the dimensionality of the problem can be reduced, PCA will find this and get the optimal solution.

Acknowledgements

We thank Prof. Wei Zhu of the State University of New York at Stony Brook for the original suggestion to use PCA. We thank Mauricio Zurita-Gotor and Prof. Daniel E. Rosner of Yale University, and Dr. Stephen E. Schwartz of BNL for encouragement and valuable discussions. This work was supported by NASA through interagency agreement number W-18,429 as part of its interdisciplinary research program on tropospheric aerosols and by the Environmental Sciences Division of the US Department of Energy, as part of the Atmospheric Chemistry Program contract DE-AC02-76CH00016.

Appendix A. Data transformation technique

The Box–Cox method (Box & Cox, 1964) is a popular way to determine transformations on variables so that, after transformation, the pdf better approximates a multivariate normal form. The method is designed for positive variables, however this is not as restrictive as it seems because a single constant can be added to each observation in the data. The method requires that a sampling of the initial pdf be available. We choose the power transformation to bring the data closer to normal form. The method transforms the variable x to $x^{(\lambda)}$ where the family of transformations indexed by λ is

$$x^{(\lambda)} = \left\{ \begin{array}{ll} \dfrac{x^\lambda - 1}{\lambda} & \lambda \neq 0 \\ \ln x & \lambda = 0 \end{array} \right\}. \tag{A.1}$$

For fixed $x > 0$, $x^{(\lambda)}$ is continuous is λ. Given the set of observations, $\{x_1, x_2, \ldots, x_n\}$, along a particular coordinate, the Box–Cox solution for λ is the one which maximizes the likelihood expression:

$$L(\lambda) = -\frac{n}{2}\ln(\mathrm{RSS}_\lambda/n) + (\lambda - 1)\sum_{i=1}^{n}\ln x_i, \tag{A.2}$$

where RSS_λ is the residual sum of squares of $x^{(\lambda)}$, that is

$$\mathrm{RSS}_\lambda = \sum_{i=1}^{n}(x_i^{(\lambda)} - \overline{x^{(\lambda)}})^2, \tag{A.3}$$

where

$$\overline{x^{(\lambda)}} = \frac{1}{n}\sum_{i=1}^{n}x_i^{(\lambda)} = \frac{1}{n}\sum_{i=1}^{n}\left(\frac{x_i^{\lambda} - 1}{\lambda}\right) \tag{A.4}$$

is the sample mean of the transformed observations.

We have also employed a simple alternative method based on moments. From the n observations, we define the new variables $z_i^{(\lambda)} = (x_i^{\lambda} - \mu_\lambda)/\sigma_\lambda$ where μ_λ and σ_λ are the mean and standard deviation of the positive distribution $\{x_i^{\lambda}\}$. By definition the expectation values for the $z^{(\lambda)}$ distribution are: $E[z^{(\lambda)}] = 0$ and $E[(z^{(\lambda)})^2] = 1$. For a normal distribution we would also have $E[(z^{(\lambda)})^3] = 0$, which is the case for any distribution $\{x_i^{\lambda}\}$ that is symmetric about μ_λ. Accordingly, we choose λ to be the exponent that minimizes $|E[(z^{(\lambda)})^3]|$.

Both methods were applied separately to the volume and area coordinates of the sampled points shown in Fig. 2a, and gave similar results: a power λ near 1/10 for volume and $-1/10$ for area. Because these exponents are not significantly different from zero, the logarithmic Box–Cox transformation (Eq. (A.1)) also gives near normal results. Both methods were applied here to statistical samplings from an initially known pdf, however, because the second method can be applied directly to moments, it has the potential advantage of enabling coordinate transformations to be updated with time even though the pdf is unknown. Fractional moments, of order dependent on the continuous parameter λ, can be estimated from the tracked moments for this purpose using polynomial interpolation methods (Frenklach, 2002; Diemer & Olson, 2002).

References

Albrecht, B. A. (1989). Aerosols, cloud microphysics, and fractional cloudiness. *Science*, *245*, 1227–1230.

Barrett, J. C., & Webb, N. A. (1998). A comparison of some approximate methods for solving the aerosol general dynamic equation. *Journal of Aerosol Science*, *29*, 31–39.

Box, G. E. P., & Cox, D. R. (1964). An analysis of transformations. *Journal of the Royal Statistical Society*, *211–243*, discussion 244–252.

Capaldo, K. P., Pilinis, C., & Pandis, S. N. (2000). A computationally efficient hybrid approach for dynamic gas/aerosol transfer in air quality models. *Atmospheric Environment*, *34*, 3617–3627.

Clegg, S. L., Brimblecombe, P., & Wexler, A. S. (1998). A thermodynamic model of the system $H^+ - NH_4^+ - SO_4^{-2} - NO_3^- - H_2O$ at tropospheric temperatures. *Journal of Physical Chemistry A*, *102*, 2137–2154.

Diemer, R. B., & Olson, J. H. (2002). A moment methodology for coagulation and breakage problems: Part 2—moment models and distribution reconstruction. *Chemical Engineering Science*, *57*, 2211–2228.

Frenklach, M. (2002). Method of moments with interpolative closure. *Chemical Engineering Science*, *57*, 2229–2239.

Jacobson, M. Z. (2001). Strong radiative heating due to the mixing state of black carbon in atmospheric aerosols. *Nature*, *409*, 695–697.

Jacobson, M. Z. (2002). Analysis of aerosol interactions with numerical techniques for solving coagulation, nucleation, condensation, dissolution, and reversible chemistry among multiple size distributions. *Journal of Geophysical Research*, *107*(D19), 4366. doi:10.1029/2001JD002044.

Koch, W., & Friedlander, S. K. (1990). The effect of particle coalescence on the surface area of a coagulating aerosol. *Journal of Colloid and Interface Science*, *140*, 419.

Marchisio, D. L., Pikturna, J. T., Fox, R. O., Vigil, D. R., & Barresi, A. A. (2003). Quadrature method of moments for population-balance equations. *A.I.Ch.E. Journal*, *49*, 1266–1276.

McGraw, R. (1997). Description of atmospheric aerosol dynamics by the quadrature method of moments. *Aerosol Science and Technology*, *27*, 255–265.

McGraw, R., & Liu, Y. (2003). Kinetic potential and barrier crossing: A model for warm cloud drizzle formation. *Physical Review Letters*, *90*, 018501.

McGraw, R., & Wright, D. L. (2003). Chemically resolved aerosol dynamics for internal mixtures by the quadrature method of moments. *Journal of Aerosol Science*, *34*, 189–209.

Meng, Z., Dabdub, D., & Seinfeld, J. H. (1998). Size-resolved and chemically resolved model of atmospheric aerosol dynamics. *Journal of Geophysical Research*, *103*, 3419–3435.

Rosner, D. E., & Pyykonen, J. (2002). Bi-variate moment method for simulation of coagulation and sintering of alumina nano-particles in flames. *A.I.Ch.E. Journal*, *4*(3), 476–491.

Rosner, D. E., McGraw, R., & Tandon, P. (2003). Multi-variate population balances via moment and Monte Carlo simulation methods. *I/EC-Research*, *42*, 2699–2711.

Seinfeld, J. H., & Pandis, S. N. (1998). *Atmospheric chemistry and physics: From air pollution to climate change*. New York: Wiley.

Twomey, S. A., Piepgrass, M., & Wolfe, T. L. (1984). An assessment of the impact of pollution on global cloud albedo. *Tellus*, *36B*, 356–366.

Wang, C.-S. (1966). *A mathematical study of the size distribution of coagulating disperse systems*. Doctoral thesis, California Institute of Technology, Pasadena, CA (p. 45).

Wilck, M. (1998). *Modal modelling of multicomponent aerosols*. Doctoral Dissertation, Leipzig University.

Wright, D. L., McGraw, R., Benkovitz, C. M., & Schwartz, S. E. (2000). Six-moment representation of multiple aerosol populations in a sub-hemispheric chemical transformation model. *Geophysical Research Letters*, *27*, 967–970.

Wright, D. L., McGraw, R., & Rosner, D. E. (2001). Bivariate extension of the quadrature method of moments for modeling simultaneous coagulation and sintering of particle populations. *Journal of Colloid and Interface Science*, *236*, 242–251.